17th Brazilian Congress of Thermal Sciences and Engineering
November 25th-28th, 2018, Águas de Lindóia, SP, Brazil

ENCIT-2018-0662
COMPUTATIONAL MODELING AND ANALYSIS OF THE CONSTRUCTIVE PARAMETERS OF A FINNED TUBE EVAPORATOR USING THE GENERATION OF ENTROPY

Henrique Neiva Guimarães
henreneivag@gmail.com

Paulo Eduardo Lopes Barbieri
baribieri@cefetmg.br

CEFET-MG, Federal Center of Technological Education of Minas Gerais, Av. Amazonas, 7675 Belo Horizonte, MG 30510-000, Brazil

Abstract. *This study aimed to improve a mathematical model, first developed by Domanski (1989) able to predict the performance of a finned tube heat exchanger trough the tube-by-tube method. To the proposed model were incorporated louvered fins, the R134a and R1234yf refrigerant, the pressure drop of air to flow between the fins and to update the correlations used to calculate the convection coefficient of airflow and refrigerant. Additionally it was incorporated to mathematical model the compute the generated entropy during operation of the equipment. The new model was validated by comparison its results with experimental results, present in the literature. An evaluation of the generation entropy number was made according evaporator's four parameters: type of fins and the distance between them, the distance between the tube rows and type of coolant. The results showed that the factors that most influence the entropy generation were the distance between the fins, the distance between the tube rows and the type of coolant, Besides that the largest share of irreversibility is associated with the flow of air between the fins.*

Keywords: *Evaporator, finned tube,, heat exchanger, entropy generation, tube-by-tube method*

1. INTRODUCTION

One of the major concerns of engineering today is the energetic efficiency, it has been sought to create equipment that consume less energy and produce fewer environmental impact. One of the equipment that consume more energy nowadays are air conditioning systems for buildings. According with Pandelidis e Anisimov (2015), between 30 and 40% of the electric energy produced in the world is spend in buildings, of which 50% is destined to ventilation and air conditioning systems. The efficiency of the air conditioning systems is directly connected to de performance of its components. The heat exchangers, essential components of the vapor compression refrigeration cycle, were extensively studied in past decades, this resulted in several mathematic models capable of simulate them. Domanski (1989) realized a numeric simulation of fined tube evaporator used one model named tube-by-tube. The results shows a maximum error in relation to the experimental value of 8.2% for the total heat capacity. Lee e Domanski (1997) used this model to evaluate the influence of the inlet air profile in the fined tube evaporator. The obtained results show that the nonuniform air distribution is capable of reduce up to 57% the total heat capacity of the evaporator when compared to a uniform distribution. Through a finite difference model, Mishra *et al.* (2008) evaluated the inlet temperature profile of the working fluids in a cross flow heat exchanger. They conclude that the variation of the inlet temperature of the cold fluid is more relevant that the hot one for the equipment efficiency. Huang *et al.* (2014) to simulate a single pipe heat exchanger created a finite volume method. The simulation considered the equipment in two different operation modes, as evaporator and condenser in cold water systems. For the system operating in the condensation mode, the model was capable to predict the total heat capacity and the pressure loss with a deviation of 5%. For the heat exchanger operating as an evaporator, the deviations were 5% for the heat capacity and 10% for the pressure loss.

Trough increasing accurate numeric models, researchers aimed to increase the efficiency of the heat exchangers, using several methods, among them the Entropy Generation Minimization (EGM) is one of the most promising. In this procedure, the entropy generation in a heat exchanger is divided in two terms, first one due the heat transfer trough finite difference temperature, the other one due the fluids pressure drop ((Bejan, 1996) ; (Hesselgreaves, 2000)). This methodology consist in reduce the entropy generation rate trough some heat exchangers parameters variation. Ye e Lee (2012) performed a study objectifying the entropy generation minimization trough the circuitry variation in a fined tube condenser. The obtained results show that the EGM methodology is capable of providing a circuitry that increase the heat exchange and reduce the entropy generation simultaneously. Pussoli *et al.* (2012) employed the EGM method to

determinate the optimum value of the peripheral finned-tube evaporators characteristic. The results pointed an optimum value of NTU that minimize the entropy generation. Zhou *et al.* (2014) used the EGM method to optimize the construction parameters in a fined plate heat exchanger.

This work aimed to simulate a fined tube evaporator through the tube-by-tube method, evaluate the entropy generation that occur during its operation as a function of four parameters: type of fins and the distance between them, the distance between the tube rows and type of coolant. In this study was employed the entropy generation number as an evaluation parameter and it was evaluated as function of the physic mechanisms that promote the irreversibility.

2. MATHEMATIC MODEL

The simulated evaporator have two identical slabs, shown in Figure 1, it was simulated using R22, R134a and R1234yf, plain, slit, louver and wave fins. The distance between fins and space between tube rows were varied from 1.0 to 16.0 mm and 15.0 to 40.0 mm respectively.

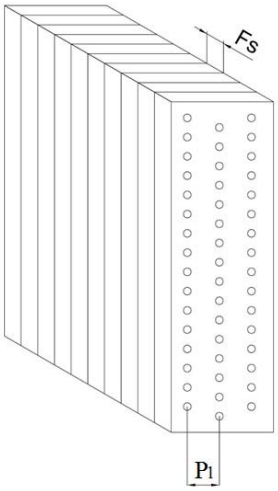

Figure 1a - Evaporator model

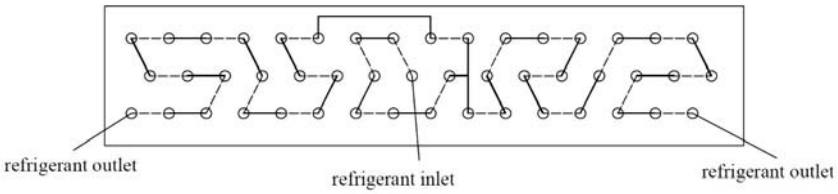

Figure 1b - Evaporator circuitry

Figure 1a show an overview of the evaporator, Figure 1b shows the circuitry employed to conduct the coolant. The boundary conditions are shown in Table 1.

Table 1 - Boundary conditions

Parameter	Valor
Slab number [-]	2
Length of tubes [mm]	454
Distance between tubes in the same row[mm]	25.4
Number of tubes in a row [-]	16
Number of rows [-]	3
Inner tube surface [-]	smooth
Outer tube diameter [mm]	10
Volumetric flow rate of air [m³/min]	31.71
Relative humidity in the inlet[-]	0.51
Refrigerant superheat in the evaporator outlet [°C]	5.6
Refrigerant quality in the evaporator inlet [-]	0.2
Air temperature in the evaporator inlet [°C]	26.7
Refrigerant temperature in the evaporator outlet [°C]	7.2

The mathematical model was based in the simulation EVSIM, proposed by Domanski (1989). However, for this study it was incorporated new correlations for heat transfer in air that flows over the fins, in addition a new kind of fin was incorporated in the model, louver fin. It was modified the correlation for convention of the coolant inside the tubes in annuli pattern, added the calculation of the pressure drop in the airside and entropy generation rate.

This method consists in the discretization of the heat exchanger in isolated tubes, each one of them, with their respective fin areas. Each tube is considered an independent heat exchanger in which their outlet conditions are used as inlet conditions of the next one, as shown in Figure 2.

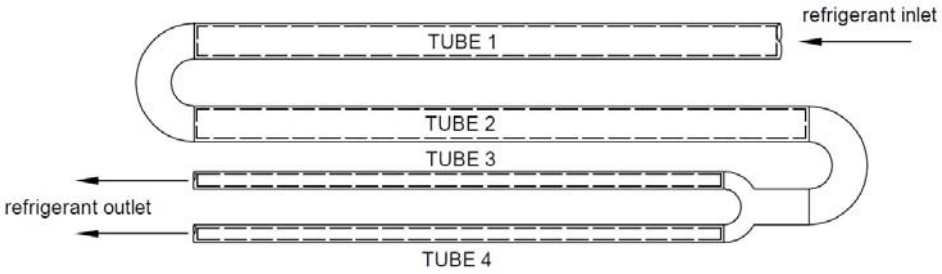

Figure 2 - Tube-by-tube method

For the calculation of the refrigerant convection coefficient, the flow was divided in three different regions according to the quality of the refrigerant: annuli (quality between 0 and 0.85), mist (quality between 0.85 and 1) and single-phase. For each regime was used a different correlation for the convection coefficient. For the annuli regime, it was employed Liu e Winterton (1991) correlation. In this formula, the overall convection coefficient (h_{an}) is express by the following equation and it is a function of forced (h_{mf}) and evaporation (h_{ev}) convection coefficient and two dimensionless parameters: E and S.

$$h_{an}^2 = \left(E\,h_{mf}\right)^2 + \left(S\,h_{ev}\right)^2 \tag{1}$$

For the evaluation of the flow in single-phase regime, it was used the Dittus-Boelter correlation, expressed below.

$$h_{mf} = 0.023 Re^{4/5} Pr^n D_{in} / k \tag{2}$$

Where D is the inner diameter, k the thermal conductivity of the refrigerant and n assume the value of 0.4.

For the calculation of the convection coefficient, when the refrigerant is in the mist regime, it was used the correlation below Domanski (1989), where x represent the refrigerant quality.

$$h_m = \left(1-x\right)h_{an} + \left(x-0.85\right)h_{mf} \tag{3}$$

The air convection coefficient is calculated trough correlations to Colburn j-factor express by the following equation for each one of the fin types.

$$j = St\ Pr^{2/3} \tag{4}$$

The used correlations are written in function of: the number of rows (N), outside tube diameter (D_{out}), distance between fins (Fs), longitudinal distance between tubes (Pl), transversal distance between tubes (PT), hydraulic diameter (Dh), collar diameter (Dc), wave angle (θ), high of the slits (Sh), width of the slit (Ss), distance between two consecutive louvers (Lp) and high of the louvers (Lh). The employed correlations are shown in Table 2. (Wang, C.-C. *et al.* (1999; Wang, C. C. *et al.* (1999; Wang *et al.* (2000; Wang *et al.* (2002)

Table 2 - Coldburn j factor correlations

Correlation	Fin model
$\begin{cases} j = 0.018 Re_{Dc}^{-0.28} \left(\frac{P_t}{P_l}\right)^{-0.15} \left(\frac{F_s}{D_c}\right)^{-1.064} \left(\frac{F_s}{D_h}\right)^{-0.184} \left(\frac{F_s}{P_t}\right)^{-0.32} & \text{if } N = 1 \\ j = 0.086 Re_{Dc}^{-0.16} N^{-0.14} \left(\frac{F_s}{D_c}\right)^{-0.37} \left(\frac{F_s}{D_h}\right)^{-0.29} \left(\frac{F_s}{P_t}\right)^{-0.052} & \text{if } N \geq 2 \end{cases}$	Flat fin
$\begin{cases} j = 0.882 Re_{Dc}^{-0.24} \left(\frac{D_c}{D_h}\right)^{-1.07} \left(\frac{F_s}{P_t}\right)^{0.52} \left(\frac{F_s}{D_c}\right)^{-0.0814} \tan(\theta)^{-0.58} & \text{for } Re_{Dc} < 1000 \\ j = 0.0646 Re_{Dc}^{-0.14} \left(\frac{D_c}{D_h}\right)^{0.48} \left(\frac{F_s}{P_t}\right)^{-1.43} \left(\frac{P_l}{D_c}\right)^{0.503} \tan(\theta)^{0.504} N^{-0.787} & \text{for } Re_{Dc} \geq 1000 \end{cases}$	Wavy fin

$$j = 1.6409 Re_{Dc}^{-1.1} \left(\frac{S_h}{S_l}\right)^{1.16} \left(\frac{P_l}{P_t}\right)^{1.87} \left(\frac{F_s}{D_c}\right)^{-2.7} N^{-0.1}$$

Slit fin

$$\begin{cases} j = 14.3117 Re_{Dc}^{-1.1} \left(\frac{F_s}{D_c}\right)^{-2.2} \left(\frac{L_h}{L_p}\right)^{-1.3} \left(\frac{F_s}{P_t}\right)^{-1.4} \left(\frac{P_l}{P_t}\right)^{-1.724} & \text{for } Re < 1000 \\ j = 1.1373 Re_{Dc}^{-0.9} \left(\frac{F_s}{P_t}\right)^{-0.8} \left(\frac{L_h}{L_p}\right)^{0.7} \left(\frac{P_l}{P_t}\right)^{-0.8} N^{0.3843} & \text{for } Re \geq 1000 \end{cases}$$

Louver fin

In order to evaluate the pressure drop in the refrigerant when flowing through the tubes, it was considered that this effect is due viscous friction and momentum variation. The equations used to procedure this calculation are pick for each configuration of flow: single-phase or multi-phase. For the single-phase regime, the pressure drop due viscous friction was modeled through the Fanning equation, as show below, where G is the mass flux, L the tube length, ρ the refrigerant density and f the friction factor.

$$\Delta P = \frac{2 f G^2 L}{D_{in} \rho} \tag{5}$$

The friction factor was obtained through the Eq.(6), Domanski (1989).

$$f = 0.046 Re^{-0.2} \tag{6}$$

The pressure drop portion due the momentum variation was obtained using the Eq. (7), Domanski (1989), where Δv is the specific volume variation.

$$\Delta P = \frac{-G^2 \Delta v}{L} \tag{7}$$

In order to evaluate the pressure drop in multi-phase regime, it was used the Pierre (1964) correlation, shown bellow. This correlation combine the friction and momentum variation effects, where x_m is the mean quality of the refrigerant in the tube, Δx the quality variation and v_m the mean specific volume.

$$\Delta P = \left(f \frac{L}{D_{in}} + \frac{\Delta x}{x_m} \right) G^2 v_m \tag{8}$$

$$f = 0.0185 \left(\frac{kf}{Re} \right)^{0.25} \tag{9}$$

$$kf = \frac{J \Delta h \, \Delta x g_c}{Lg} \tag{10}$$

Where g is the gravity acceleration, Δh the latent vaporization heat, gc is 9.81 and J is 4.184.
In order to evaluate the air pressure drop, it was used the Eq.(11), Domanski (1989).

$$\Delta P = \frac{2 f G^2 A}{4 A_c \rho} \tag{11}$$

In which A is the total heat transfer area, Ac the minimum flow area, ρ the air density and f the friction factor. This last term represent simultaneously the pressure drop due viscous friction and momentum variation, as shown in Eq. (12), Wang *et al.* (2015).

$$f = \frac{A_c}{A}\frac{\rho_m}{\rho_{in}}\left[\frac{2\Delta P \rho_{in}}{G^2} - \left(1+\sigma^2\right)\left(\frac{\rho_{in}}{\rho_{out}} - 1\right)\right] \tag{12}$$

Where ρ_m is the air mean density and σ is the contraction ratio of cross-sectional area. In order to calculate the friction factor for each kind of fin were used the correlations shown in Table 3. (Wang, C.-C. *et al.* (1999; Wang, C. C. *et al.* (1999; Wang *et al.* (2000; Wang *et al.* (2002)

Table 3 - Friction factor correlation

Correlation	Fin model
$f = 0.0267\, Re_{Dc}^{f_1} \left(\frac{F_s}{F_l}\right)^{f_2} \left(\frac{F_s}{D_c}\right)^{f_3}$	Flat fin
$\begin{cases} f = 4.37 Re_{Dc}^{f_1} \left(\frac{F_s}{D_h}\right)^{f_2} \left(\frac{F_l}{P_t}\right)^{f_3} \left(\frac{D_c}{D_h}\right)^{0.2284} N^{f_4} & \text{for } Re_{Dc} < 1000 \\ f = 0.228 Re_{Dc}^{f_5} (\tan\theta)^{f_6} \left(\frac{F_s}{F_l}\right)^{f_7} \left(\frac{F_l}{D_c}\right)^{f_8} \left(\frac{D_c}{D_h}\right)^{0.188} \left(\frac{P_t}{P_l}\right)^{-0.547} & \text{for } Re_{Dc} \geq 1000 \end{cases}$	Wavy fin
$f = 0.1851\, Re_{Dc}^{f_1} \left(\frac{F_s}{D_c}\right)^{f_2} \left(\frac{S_s}{S_h}\right)^{f_3} N^{-0.046}$	Slit fin
$\begin{cases} f = 0.00317 Re_{Dc}^{f_1} \left(\frac{F_s}{F_l}\right)^{f_2} \left(\frac{D_h}{D_c}\right)^{f_3} \left(\frac{L_h}{L_p}\right)^{f_4} \left(\ln\left(\frac{A_0}{A_t}\right)\right)^{-0.0488} & \text{for } N = 1 \\ f = 0.06393 Re_{Dc}^{f_5} \left(\frac{F_s}{D_c}\right)^{f_6} \left(\frac{D_h}{D_c}\right)^{f_7} \left(\frac{L_h}{L_p}\right)^{f_8} N^{f_9} (\ln(Re_{Dc}) - 4)^{-1.092} & \text{for } N > 1 \end{cases}$	Louver fin

2.1 Entropy evaluation

In order to calculate the entropy generation during the equipment operation, the evaporator was modeled as a control volume, as shown in Figure 3.

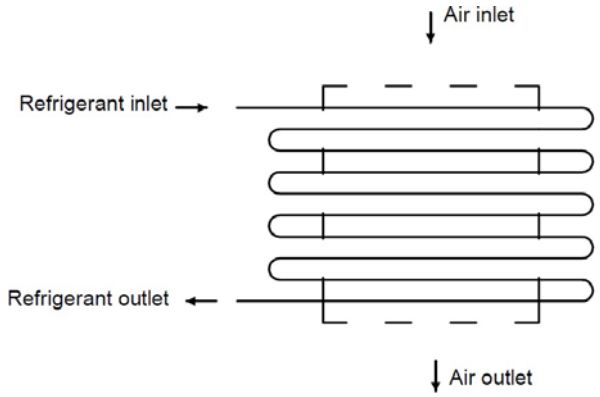

Figure 3 - Evaporator as a control volume

The entropy generation was divided in two terms one due heat transfer and the other due pressure drop for each one of the working fluids, as show in Eq. (13). After the analyses of each portion of the entropy generation, they were summed to obtain the overall entropy generation rate, as shown in Eq. (14).

$$\dot{S}_{gen} = \frac{\dot{Q}\Delta T}{T_{ref} T_{air}} + \frac{\dot{m}\Delta P}{T\rho} \tag{13}$$

$$\dot{S}_{gen\ tot} = \dot{S}_{\Delta T} + \dot{S}_{\Delta P\ ar} + \dot{S}_{\Delta P\ ref} \tag{14}$$

In witch $\dot{Q}$ is the heat exchanged, ΔT the temperature difference between the working fluids, ΔP the overall pressure drop, T_ref e T_air the mean temperature of the refrigerante and air respectively. The ΔT and ΔP index in Eq. (14) denote the entropy generation hate due heat transfer and pressure drop respectively. The value of T in the second term in the right of Eq. (13) denote the analyzed fluid temperature, air or refrigerant.

For the evaluation of the constructive parameters as a function of the entropy generation rate, it was used the generation entropy number (Ns), as proposed by Ye e Lee (2012). This dimensionless parameter, shown in Eq. (15), expresses the relation between the generation entropy that occurs and a characteristic entropy generation value due heat transfer.

$$Ns = \frac{\dot{S}_{gen} T_t}{\dot{Q}} \tag{15}$$

Where S_{gen} is the entropy generation rate, Tt the heat transfer temperature and $\dot{Q}$ the heat flux.

3. RESULTS AND DISCUSSION

The validation of the model was made by comparing the obtained values for heat capacity with experimental values. The data used in the comprising were obtained by Chwalowski *et al.* (1989) through tests in real equipment, in this study, was analyzed the behavior of the evaporator with different inclinations in relation (25°, 45°, 65° e 90°) with the duct, as shown in Figure 4.

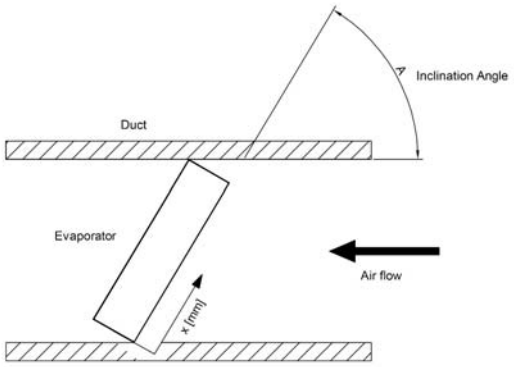

Figure 4 - Evaporator inclination

The different inclinations resulted in several different velocity profiles, shown in Figure 5. The developed model for wavy fins was subjected to the velocity profiles in Figure 5 and the boundary conditions shown in Table 4, used for Chwalowski *et al.* (1989).

Table 4 - Test Conditions

Inclination	Volumetric air flow rate	Air dry bulb temperature	Air wet bulb temperature	Refrigerant saturation temperature in evaporator outlet	Refrigerant superheat in the evaporator outlet
25°	15.80 m³/min	26.6 °C	19.4°C	7.2°C	4.8°C
45°	16.10 m³/min	26.6 °C	19.4°C	7.2°C	4.3°C
65°	16.00 m³/min	26.6 °C	19.4°C	7.2°C	5.8°C
90°	16.00 m³/min	26.6 °C	19.4°C	7.2°C	3.0°C

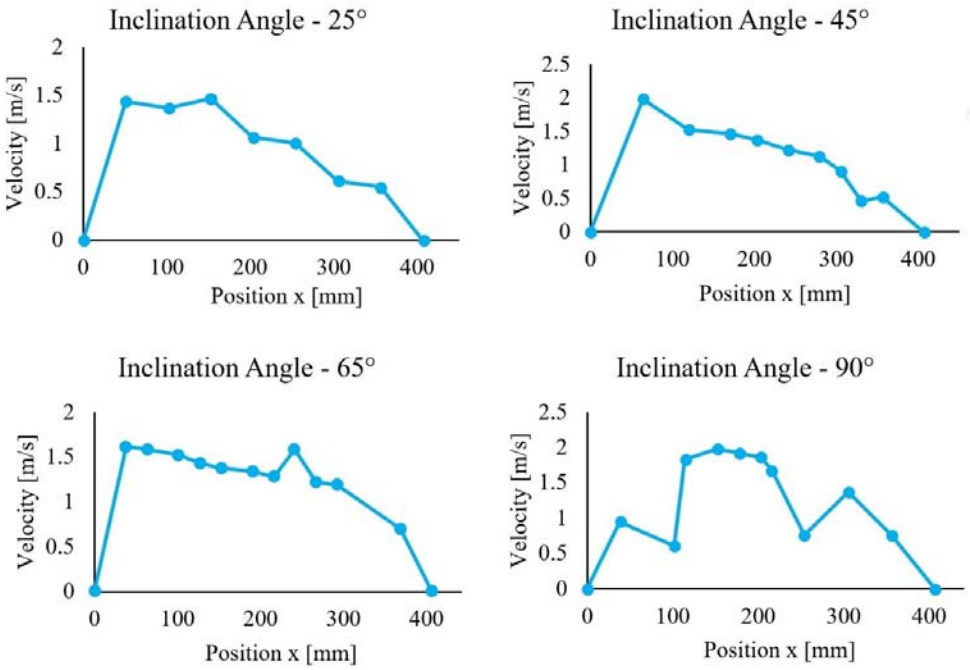

Figure 5 - Air inlet velocity profiles

The results and the analyze made with them are show below, they are divided according to the analyzed parameters in order to facilitate the visualization of their influence on the entropy generation. Due the similarity of the results that some parameters combinations exhibit, was chose only one to be discussed in each item. The presented results are capable to describe other combinations.

The latent and overall heat capacity was then confronted with the experimental data, as showed in Figure 6. The results show a maximum discrepancy of 12.8% for the overall heat capacity and 24.7% for the latent capacity.

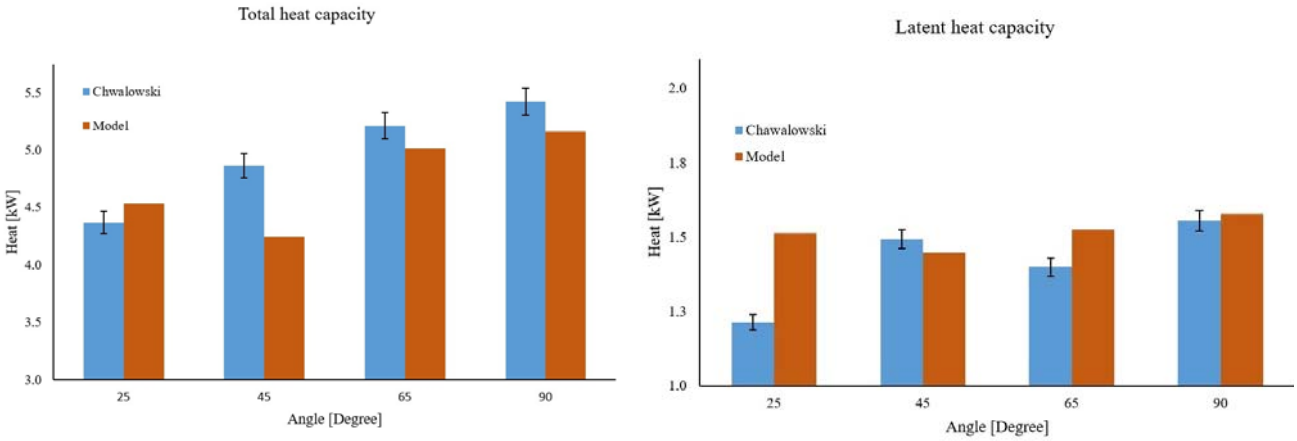

Figure 6 - Model validation

The kind of fin used in the evaporator was a crucial parameter for the entropy generation during the equipment operation. Figure 7 show the value of Ns associated with each fin model when the evaporator is operating with R1234yf. As can be seen, the evaporator that contains louver fins is the one that have more irreversibility associated with their operation. In addition, is possible to see that the major part of the entropy generation for all the tested fins are due the pressure drop. For the wavy fins, that present the smallest irreversibility share, 80% of the Ns is due the pressure drop. For the Louver fin, this share is 87%. Analyzing the entropy generation number exclusively due the pressure drop it is possible to notice that the Ns due the refrigerant flow is similar in both fin models, although the share originated by the air flow is different in each case, being bigger in the louver fin.

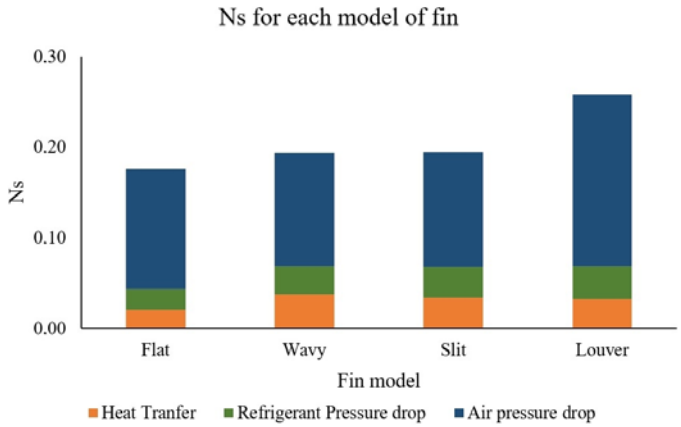

Figure 7 - Ns for each fin model

The irreversibility share generated by the airflow is the reason why the louver fin have a bigger overall Ns, as shown in Figure 7. This occur, because, the presence of the louver structure promote the destruction of the boundary layer in order to improve the heat transfer. However, these structures also act like a resistance to the airflow, resulting in a higher pressure drop.

Among the analyzed coolants, the one that stood as the best option in terms of irreversibility was the R22, followed by R134a and R1234yf. As can be seeing in Figure 8, the refrigerant R22 generate a smaller Ns and the value for R134a and R1234yf are very close. The values for Ns associated with heat transfer and pressure drop in the airflow are very close in the three types of coolant tested. The value that differ their irreversibility generation are the pressure drop for the refrigerant. The value obtained for this parameter with R134a and e1234yf are very close. Although this amount of irreversibility for R22 are approximately half of that value obtained for the other coolants. The main reason for this behavior is that, for the same condition, the R22 specific volume as superheated vapor is smaller than for r1234yf and R134a. This difference cause a lower pressure drop for the R22 flow when compared with R1234yf and R134a and consequently a lower Ns due refrigerant pressure drop.

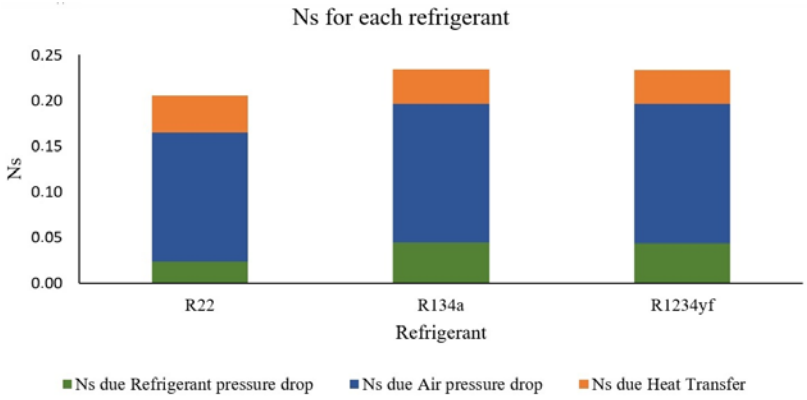

Figure 8 - Ns for each refrigerant

Due to the high degree of coupling of the parameters distance between the fins and distance between the rows of tubes, these characteristics were analyzed together. The flat, slit and louver fins had an optimum spacing between them which minimized the irreversibility during the operation of the equipment. The wavy fins, in turn, do not exhibit such behavior, the number of entropy generation drops in an asymptotic shape with the increase in the distance between the fins as shown in Figure 9.

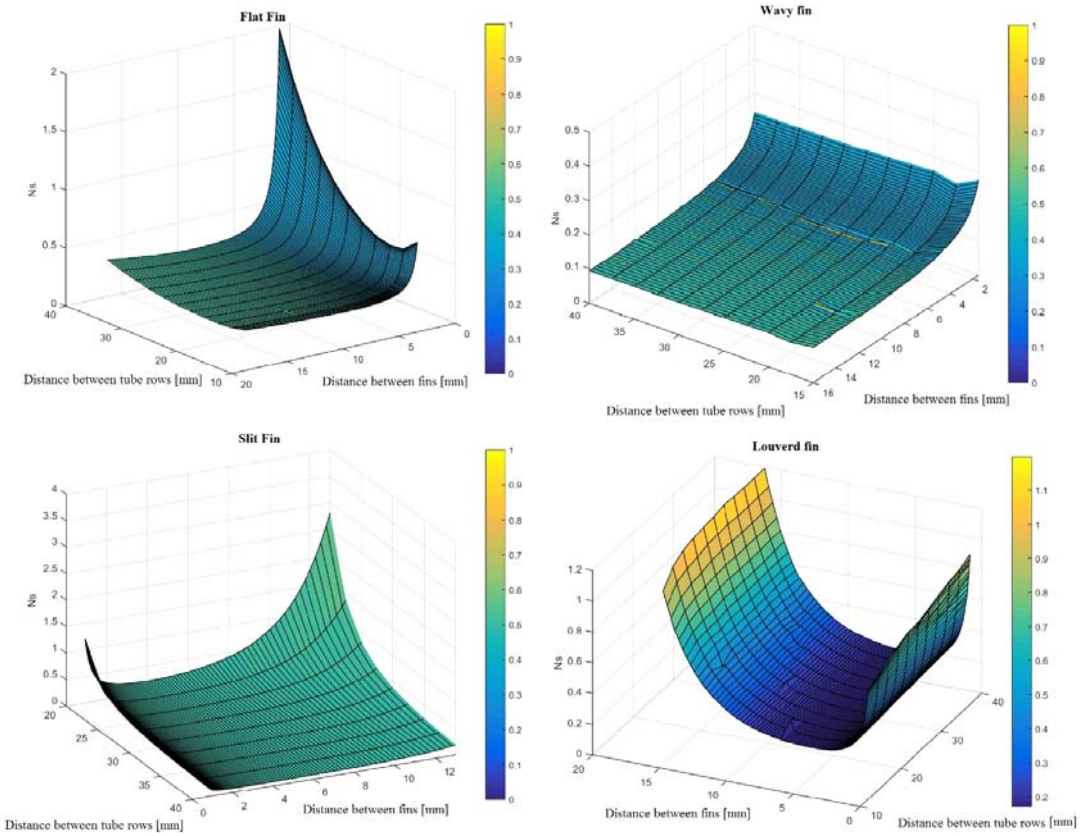

Figure 9 - Ns for different distance between fins and tube row

As can be seen from Figure 9, the behavior presented by Ns is different when the distance between the fins and the distance between the rows of tubes is varied. The changes in the distance between consecutive rows do not impose major changes in the number of entropy generation, except for the flat and slit fins. The change in the distance between the fins in turn, brings about major changes in Ns. The flat and louver fins present a curve that makes it possible to determine the spacing between the fins that provides the smaller number of entropy generation. The slit fins have values of Ns that decrease rapidly when the distance between the rows of tubes is small, but does not present large variations in its value when the distance of the fins assumes larger values. Louver and wavy fin types do not show significant variations in the number of entropy generation when the distance between rows of tubes changes.

The asymptotic behavior shown for the entropy generation number of the wavy fins in relation to the distance between them can be attributed to the distribution of the physical mechanisms that cause irreversibility. As shown in Figure 10, the increasing in the distance between the fins alters the proportion of the physical effects that cause entropy generation. When the distance between the fins is 1.5 mm the mechanism that promotes greater irreversibility is the pressure drop (82%). However, when this distance is 15 mm, the heat transfer is responsible for 52% of the generated irreversibility. As the distance between the fins increases the constraint imposed on the airflow decreases, which causes the entropy generated by this physical mechanism to also be reduced to a point where it stabilizes. This behavior of the pressure drop is only observed in the wavy fins, in the other types of fins there is a critical point in which a minimum value of Ns occurs due to this phenomenon so that it increases again.

The different behavior of the wavy fin can be explained by the low influence that the boundary layer appears to have on the flow as a whole as the distance of the fins increases. The number of entropy generation due to heat transfer increases noticeably as the distance between the fins becomes larger, and tends to stabilize for long distances. This effect can be explained by the reduction of the heat transfer area that the evaporator undergoes, as the distance between the fins increases. With a smaller heat exchange area, the heat capacity of the heat exchanger decreases, stabilizing for long distances between the fins. With the reduction of the heat transfer between the refrigerant and the air, the evaporator's air outlet temperature increases until it stabilizes for high distance values between the fins, this is the reason why the Ns due to heat transfer to follow the asymptotic behavior shown in Figure 10.

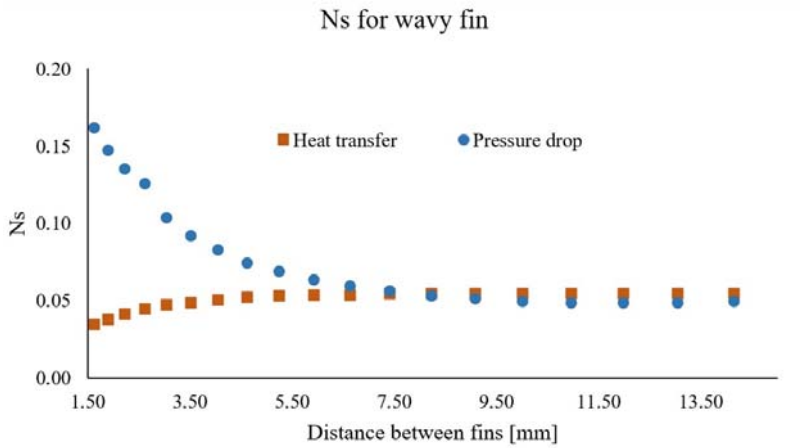

Figure 10 - Ns as a function of distance between fins for wavy fin

The influence of the distance between consecutive rows of tubes in the number of entropy generation is low when compared to the distance between the fins, as can be seen in Figure 9. As can be seen in Figure 11, the entropy generation rate by the evaporator with flat, wavy and louver fins undergoes a small rise with increasing distance between the rows of tubes. The entropy associated with the pressure drop becomes greater with the increase in the distance between the rows. This effect is explained by the hydraulic behavior downstream the tube, when the tube rows are close, the wake region exert a big influence in next tubes, exposing them to a low velocity flow. When the tube rows are distant, the wake region have less influence in the downstream flux, in this way, the next tubes are exposed to a high velocity flow, increasing the pressure drop in the equipment. The rise of the entropy generated rate due pressure drop cause the increasing of total entropy generation rate in the equipment, as shown in Figure 11.

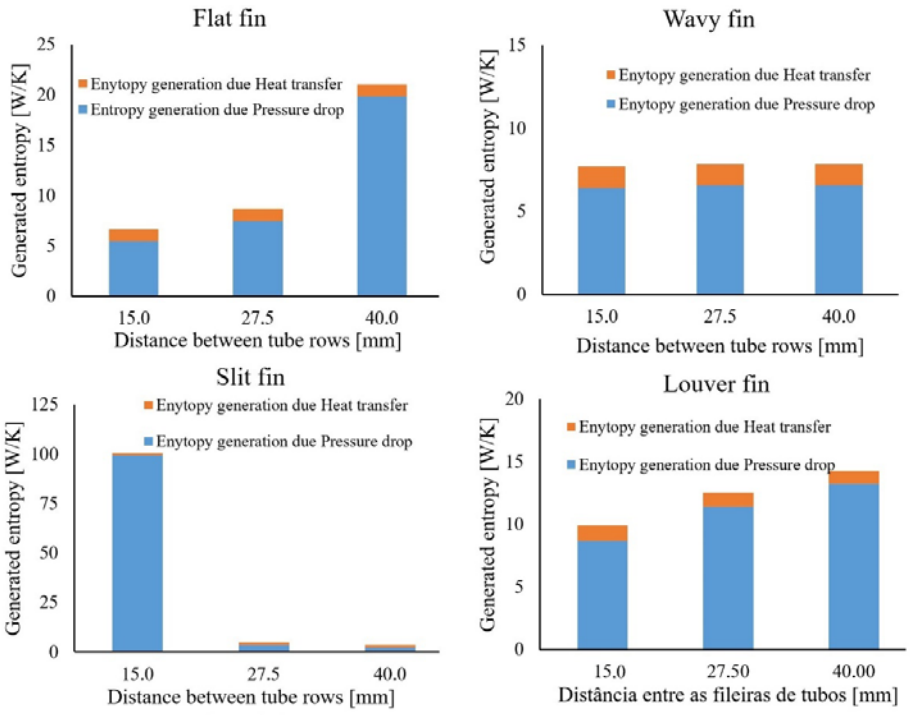

Figure 11 - Entropy generation rate as a function of distance between tube rows

In addition, the heat transferred increase with the increment in the distance between the tube rows as showed in Figure 12. This behavior is explained by the higher velocity of the airflow that promote a larger convection coefficient. As the entropy generation rate and the heat transferred both increase with the increment of the tube rows distance, a compensation between these two values occur. This behavior would tend to stabilize the number of entropy generation, which explains the low variation that it presents.

The behavior observed for the slit fin is different from that observed in the other types of fins. As the distance between the tubes rows increases, there is a noticeable decrease in the heat exchanged, as shown in Figure 12, which

causes the number of entropy generation attributed to the heat transfer to increase very little. Due to the low variation it undergoes, the generation of entropy caused by the heat transfer of, the phenomenon that determines the generation of total entropy is the pressure drop. As can be seen in Figure 11, the entropy generated by the pressure drop for this type of fin decreases sharply at low distances between the rows of tubes and stabilizing for spacing between the larger rows.

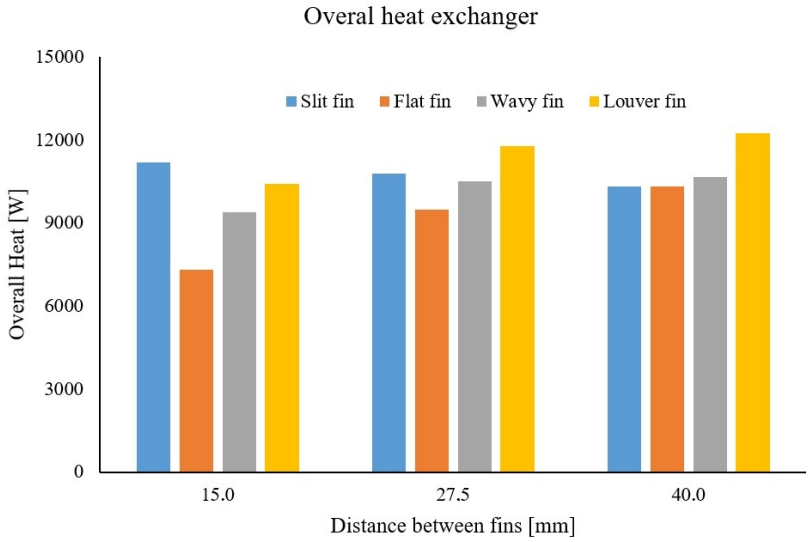

Figure 12 - Heat exchanged as a function of distance between tube rows

4. CONCLUSION

Analyzing the obtained results, it may be noted that among the four tested parameter evaluated in this work, those that showed major influence in the entropy generation number were the fin model, distance between fins and the refrigerant employed as working fluid. The distance between consecutive rows showed little influence in the entropy generation with the exception of slit and flat fins when the distance between then are small.

In addition, it was possible to perceive that the physical phenomenons that contribute most in the entropy generation during the equipment operation is the airflow pressure drop. The exception was the evaporator with wavy fins and large distance between them, this configuration exhibit heat transfer as the major contribution on the irreversibility formation.

The analyze present in this study demonstrate that the difference between the entropy generation number associated with R134a and R1234yf is negligible, for this reason, it is therefore recommended to use the latter because it is more environmentally friendly.

5. ACKNOWLEDGEMENTS

The authors would like to extend the acknowledgement to the CAPES by the financial support given to the present investigation.

6. REFERENCES

BEJAN, A. **Entropy Generation Minimization: The method of thermodynamic Optimization of Finite-Size System and Finite-time Processes**. Boca Raton: CRC Press, 1996.

CHWALOWSKI, M.; DIDION, D. A.; DOMANSKI, P. A. Verification of Evaporator Computer Models and Analysis of Performance of an Evaporator Coil. **ASHRAE Transactions,** v. 95, p. 1229-1236, 1989.

DOMANSKI, P. A. **EVSIM an evaporator simulation model accounting for refrigerant and one dimensional air distribution**. NIST report. 1989

HESSELGREAVES, J. E. Rationalization of second law analysis of heat exchangers. **International Journal of Heat and Mass Transfer,** v. 43, p. 4189-4204, 2000.

HUANG, L.; AUTE, V.; RADERMACHER, R. A finite volume coaxial heat exchanger model with moving boundaries and modifications to correlations for two-phase flow in fluted annuli. **International Journal of Refrigeration,** v. 40, p. 11-23, 2014.

LEE, J.; DOMANSKI, P. **Impact of Air and Refrigerant Maldistributions On the Performance of Finned-Tube Evaporators With R-22 and R-407C**. National Institute of Standards and Technology - NIST. Gaithersburg, Maryland. 1997

LIU, Z.; WINTERTON, R. H. S. A general correlation for saturated and subcooled flow boiling in tubes and annuli, based on a nucleate pool boiling equation. **International Journal of Heat and Mass Transfer,** v. 34, n. 11, p. 2759-

2766, 1991/11/01/ 1991. ISSN 0017-9310. Disponível em: < http://www.sciencedirect.com/science/article/pii/0017931091902346 >.

MISHRA, M.; DAS, P. K.; SARANGI, S. Effect of temperature and flow nonuniformity on transient behaviour of crossflow heat exchanger. **International Journal of Heat and Mass Transfer,** v. 51, p. 2583-2592, 2008.

PANDELIDIS, D.; ANISIMOV, S. Numerical analysis of the heat and mass transfer processes in selected M-Cycle heat exchangers for the dew point evaporative cooling. **Energy Conversion and Management,** v. 90, p. 62-83, 2015.

PIERRE, B. Flow resistance with boiling refrigerants. **ASHRAE Journal,** v. 06, p. 58-65, 1964.

PUSSOLI, B. F. et al. Optimization of peripheral finned-tube evaporators using entropy generation minimization. **International Journal of Heat and Mass Transfer,** v. 55, n. 25, p. 7838-7846, 2012/12/01/ 2012. ISSN 0017-9310. Disponível em: < http://www.sciencedirect.com/science/article/pii/S0017931012006424 >.

WANG, C.-C.; CHEN, K.-Y.; LIN, Y.-T. Investigation of the semi-dimple vortex generator applicable to fin-and-tube heat exchangers. **Applied Thermal Engineering,** v. 88, p. 192-197, 2015/09/05/ 2015. ISSN 1359-4311. Disponível em: < http://www.sciencedirect.com/science/article/pii/S1359431114008266 >.

WANG, C.-C.; CHI, K.-Y.; CHANG, C.-J. Heat transfer and friction characteristics of plain fin-and-tube heat exchangers, part II: Correlation. **International Journal of Heat and Mass Transfer,** v. 43, n. 15, p. 2693-2700, 2000/08/01/ 2000. ISSN 0017-9310. Disponível em: < http://www.sciencedirect.com/science/article/pii/S0017931099003336 >.

WANG, C.-C.; HWANG, Y.-M.; LIN, Y.-T. Empirical correlations for heat transfer and flow friction characteristics of herringbone wavy fin-and-tube heat exchangers. **International Journal of Refrigeration,** v. 25, n. 5, p. 673-680, 2002/08/01/ 2002. ISSN 0140-7007. Disponível em: < http://www.sciencedirect.com/science/article/pii/S0140700701000494 >.

WANG, C.-C.; TAO, W.-H.; CHANG, C.-J. An investigation of the airside performance of the slit fin-and-tube heat exchangers. **International Journal of Refrigeration,** v. 22, n. 8, p. 595-603, 1999/12/01/ 1999. ISSN 0140-7007. Disponível em: < http://www.sciencedirect.com/science/article/pii/S0140700799000316 >.

WANG, C. C. et al. Heat transfer and friction correlation for compact louvered fin-and-tube heat exchangers. **International Journal of Heat and Mass Transfer,** v. 42, n. 11, p. 1945-1956, 1999/06/01/ 1999. ISSN 0017-9310. Disponível em: < http://www.sciencedirect.com/science/article/pii/S0017931098003020 >.

YE, H. Y.; LEE, K. S. Refrigerant circuitry design of fin-and-tube condenser based on entropy generation minimization. **International Journal of Refrigeration,** v. 35, p. 1430-1438, 2012.

ZHOU, Y. et al. Optimization of plate-fin heat exchangers by minimizing specific entropy generation rate. **International Journal of Heat and Mass Transfer,** v. 78, p. 942-946, 2014/11/01/ 2014. ISSN 0017-9310. Disponível em: < http://www.sciencedirect.com/science/article/pii/S0017931014006425 >.

7. RESPONSIBILITY NOTICE

The author(s) is (are) the only responsible for the printed material included in this paper.